Supplementary Information

DNA-Based Cooperative Games: An Interactive Collective Decision-Making Architecture

Yao Yao,[a, b] Xiaokang Zhang,[a, b] Ranfeng Wu,[a, b] Shuang Cui,[a, b] Lijun Sun,[a, b] Bin Wang,[c] Qiang Zhang [a, b *]

[a] *School of Computer Science and Technology, Dalian University of Technology, Dalian, 116024, Liaoning, China*

[b] *Key Laboratory of Social Computing and Cognitive Intelligence (Dalian University of Technology), Ministry of Education, Dalian, 116024, Liaoning, China*

[c] *Key Laboratory of Advanced Design and Intelligent Computing (Dalian University), Ministry of Education, Dalian, 116622, Liaoning, China*

*Corresponding author: Qiang Zhang

E-mail address: zhangq@dlut.edu.cn

Further details, such as experiment instruments, chemical materials, DNA sequences, additional experimental results, and supplementary findings, are provided in the supporting PDF.

Contents

Table S1. Experiment instruments and chemical materials.

Name	Supplier	Identifier
NanoDrop 2000 Spectrophotometer	ThermoFisher Scientific Inc., USA	Cat#: ND-2000
C1000 Touch™ Thermal Cycler with 96-Well Fast Reaction Module	Bio-Rad Inc., USA	Cat#: 851196
Tecan Spark	Tecan Trading AG, Switzerland	Cat#: 30086376
DYCZ-24DN Mini Dual Vertical Electrophoresis Instrument	Beijing Liuyi Biotechnology Co., Ltd., China	Cat#: 121-2446
Ammonium persulfate	Sinopharm Chemical Reagent Co., Ltd., China	Cat#: 10002618
Sodium hydroxide	Sinopharm Chemical Reagent Co., Ltd., China	Cat#: 10019762
Formamide	Sinopharm Chemical Reagent Co., Ltd., China	Cat#: 30091218
Magnesium acetate tetrahydrate	Sinopharm Chemical Reagent Co., Ltd., China	Cat#: 30110518
N,N,N',N'-Tetramethylethylenediamine (TEMED)	Sinopharm Chemical Reagent Co., Ltd., China	Cat#: 80125336
Glacial acetic acid	Sinopharm Chemical Reagent Co., Ltd., China	Cat#: 10000208
Ethylenediamine tetraacetic acid disodium salt dehydrate (EDTA-$Na_2 \cdot 2H_2O$)	Sigma-Aldrich, Germany	Cat#: E5134
Tris	Sangon Biotech (Shanghai) Co., Ltd., China	Cat#: A610195
Stains-all	Sangon Biotech (Shanghai) Co., Ltd., China	Cat#: A606359
Acrylamide	Sangon Biotech (Shanghai) Co., Ltd., China	Cat#: A501033
Bis-acrylamide	Sangon Biotech (Shanghai) Co., Ltd., China	Cat#: A100172
Lambda exonuclease, 10× reaction buffer	New England Biolabs (Beijing) Ltd., China	Cat#: M0262L

The table contains all the experimental instruments and chemical materials required for this article.

Table S2. DNA sequences for TDM mechanism.

Name	Sequence 5'-3'
C	**PO_4**-CAACTCAATCACACATATCACCATTCCATATCTTTCACCTCCTCCAACAC
S	GTGTTGGAGGAGGTGAAAGATATGGAATGG
P	TGATATGTGTGATTGAGTTGAATTAATTAA
TA	TGATATGTGTGATTGAGTTGATATGGGAATAGTGATGAGAAGTGTTTAAG
TB	GTTAGTGTAAGTAGTAGTTGAGTAGGATGATGATGTCACTATTCCCATAT
TC	GTAGTATGAATTAGGTAGATCTTAAACACTTCTCACATCATCATCCTACT
VA	CTTAAACACTTCTCATCACTATTCCCATATCAACTCAATCACACATATCA
VB	ATATGGGAATAGTGACATCATCATCCTACTCAACTACTACTTACACTAAC
VC	AGTAGGATGATGATGTGAGAAGTGTTTAAGATCTACCTAATTCATACTAC
RR	**ROX**-ATGGAAAGAGTTGGAAGGGTTTGCTCTTTCCATGTGTTGGAGGAGGTGAAAGA
RQ2	CCATTCCATATCTTTCACCTCCTCCAACAC-**BHQ2**

Related to Figures 1 and S2–S12.

Due to the fact that not every experiment reconstructs DNA sequences, some sequences may be used across experiments. Therefore, there are overlapping sequences in the table below, which will not be described again in the future.

Table S3. DNA sequences for signal interference experiment.

Name	Sequence 5'-3'
C	**PO_4**-CAACTCAATCACACATATCACCATTCCATATCTTTCACCTCCTCCAACAC
S	GTGTTGGAGGAGGTGAAAGATATGGAATGG
P	TGATATGTGTGATTGAGTTGAATTAATTAA
TA	TGATATGTGTGATTGAGTTGATATGGGAATAGTGATGAGAAGTGTTTAAG
TB	GTTAGTGTAAGTAGTAGTTGAGTAGGATGATGATGTCACTATTCCCATAT
TC	GTAGTATGAATTAGGTAGATCTTAAACACTTCTCACATCATCATCCTACT
VA	CTTAAACACTTCTCATCACTATTCCCATATCAACTCAATCACACATATCA
VB	ATATGGGAATAGTGACATCATCATCCTACTCAACTACTACTTACACTAAC
VC	AGTAGGATGATGATGTGAGAAGTGTTTAAGATCTACCTAATTCATACTAC
VD	ACTCTACTGAATCTATATATACATATAACATTCTATCCATCTCACATCTA
VE	CGCTACACCGTACTCACTAACTCACCTCTGCACCAGCTCTTATCTTACTT
VF	ATACTCTTGAATTTCTTCCATCATATTAAGTCCACTACTTCCAAACCTTA
VG	CTAACTTCATTCTACTTATAAATCCTCATTAGTTCCTCTATCCTACCTAC
VH	ATTATCTACAATATTCTATATTACATCTAACTACATTCATCTCTTATATC
RR	**ROX**-ATGGAAAGAGTTGGAAGGGTTTGCTCTTTCCATGTGTTGGAGGAGGTGAAAGA
RQ2	CCATTCCATATCTTTCACCTCCTCCAACAC-**BHQ2**

Related to Figures 1 and S13–S17.

Table S4. DNA sequences for TDM-O.

Name	Sequence 5'-3'
CR	**PO_4**-CAAACCTAACTAACCTTAACCCATTCCATATCTTTCACCTCCTCCAACAC
S	GTGTTGGAGGAGGTGAAAGATATGGAATGG
TAR	GTTAAGGTTAGTTAGGTTTGATATGGGAATAGTGATGAGAAGTGTTTAAGGAGTGTTAGTAATGA
TBR	GTTAAGGTTAGTTAGGTTTGGTAGAGATGATGATGTCACTATTCCCATATAGTAGATAAGTAGTA
TCR	GTTAAGGTTAGTTAGGTTTGCTTAAACACTTCTCACATCATCATCTCTACACATTATTACATCAT
VAR	TCATTACTAACACTCCTTAAACACTTCTCATCACTATTCCCATATCAAACCTAACTAACCTTAAC
VBR	TACTACTTATCTACTATATGGGAATAGTGACATCATCATCTCTACCAAACCTAACTAACCTTAAC
VCR	ATGATGTAATAATGTGTAGAGATGATGATGTGAGAAGTGTTTAAGCAAACCTAACTAACCTTAAC
VARO	TCATTACTAACACTCCTTAAACACTTCTCATCACTATTCCCATAT
VBRO	TACTACTTATCTACTATATGGGAATAGTGACATCATCATCTCTAC
VCRO	ATGATGTAATAATGTGTAGAGATGATGATGTGAGAAGTGTTTAAG
RR	**ROX**-ATGGAAAGAGTTGGAAGGGTTTGCTCTTTCCATGTGTTGGAGGAGGTGAAAGA
RQ2	CCATTCCATATCTTTCACCTCCTCCAACAC-**BHQ2**

Related to Figures 3, S18 and S19.

Table S5. DNA sequences for TDM-A.

Name	Sequence 5'-3'
CN	**PO_4**-CAACTCAATCACACATATCACATCTACTCACTACTCTAACTACTTAGTGAGTAGATGCCATTCCATATCTTTCACCTCCTCCAACAC
S	GTGTTGGAGGAGGTGAAAGATATGGAATGG
N	CATCTACTCACTAAGTAGTTAGAGTAGTGAGTAGATGTTATTTTATTTTATTTTATTT
VN	AATAAAATAAAATAAAATAACATCTACTCACTACTCTAACTACTTAGTGAGTAGATG
TA	TGATATGTGTGATTGAGTTGATATGGGAATAGTGATGAGAAGTGTTTAAG
TB	GTTAGTGTAAGTAGTAGTTGAGTAGGATGATGATGTCACTATTCCCATAT
TC	GTAGTATGAATTAGGTAGATCTTAAACACTTCTCACATCATCATCCTACT
VA	CTTAAACACTTCTCATCACTATTCCCATATCAACTCAATCACACATATCA
VB	ATATGGGAATAGTGACATCATCATCCTACTCAACTACTACTTACACTAAC
VC	AGTAGGATGATGATGTGAGAAGTGTTTAAGATCTACCTAATTCATACTAC
RR	**ROX**-ATGGAAAGAGTTGGAAGGGTTTGCTCTTTCCATGTGTTGGAGGAGGTGAAAGA
RQ2	CCATTCCATATCTTTCACCTCCTCCAACAC-**BHQ2**

Related to Figures 4, S20–S23.

Table S6. DNA sequences for TDM-R.

Name	Sequence 5'-3'
CW	**PO_4**-CAACTCAATCACACATATCACCATTCCATATCTTTCACCTCCTCCAACACATCTCATTCCATCATA CTACATGGAAAGAGTTGGAAGGGTTTGCTCTTTCCATGTGTTG
S	GTGTTGGAGGAGGTGAAAGATATGGAATGG
SW	CAACACATGGAAAGAGCAAACCCTTCCAACTCTTTCCAT-**BHQ2**
W	GATTAGTAAGGTAGTATGATGGAATCACTCTATCACTACTCTTCATACTTAGTGATAGAGTGGAGAT
P	TGATATGTGTGATTGAGTTGTTATTTTATT
Vw	ATCTCATTCCATCATACTACCTTACTAATC
Pw	GTAGTATGATGGAATGAGATTTATTTTATT
TA	TGATATGTGTGATTGAGTTGATATGGGAATAGTGATGAGAAGTGTTTAAG
TB	GTTAGTGTAAGTAGTAGTTGAGTAGGATGATGATGTCACTATTCCCATAT
TC	GTAGTATGAATTAGGTAGATCTTAAACACTTCTCACATCATCATCCTACT
VA	CTTAAACACTTCTCATCACTATTCCCATATCAACTCAATCACACATATCA
VB	ATATGGGAATAGTGACATCATCATCCTACTCAACTACTACTTACACTAAC
VC	AGTAGGATGATGATGTGAGAAGTGTTTAAGATCTACCTAATTCATACTAC
RR	**ROX**-ATGGAAAGAGTTGGAAGGGTTTGCTCTTTCCATGTGTTGGAGGAGGTGAAAGA
RQ2	CCATTCCATATCTTTCACCTCCTCCAACAC-**BHQ2**

Related to Figures 5, S24 and S25.

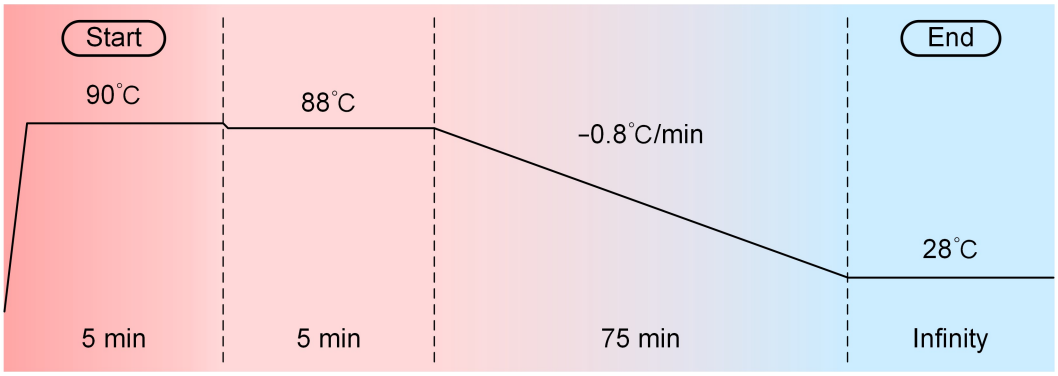

Figure S1. Annealing program (related to all experiments).

All DNA structures requiring annealing in this study were subjected to this simple annealing procedure.

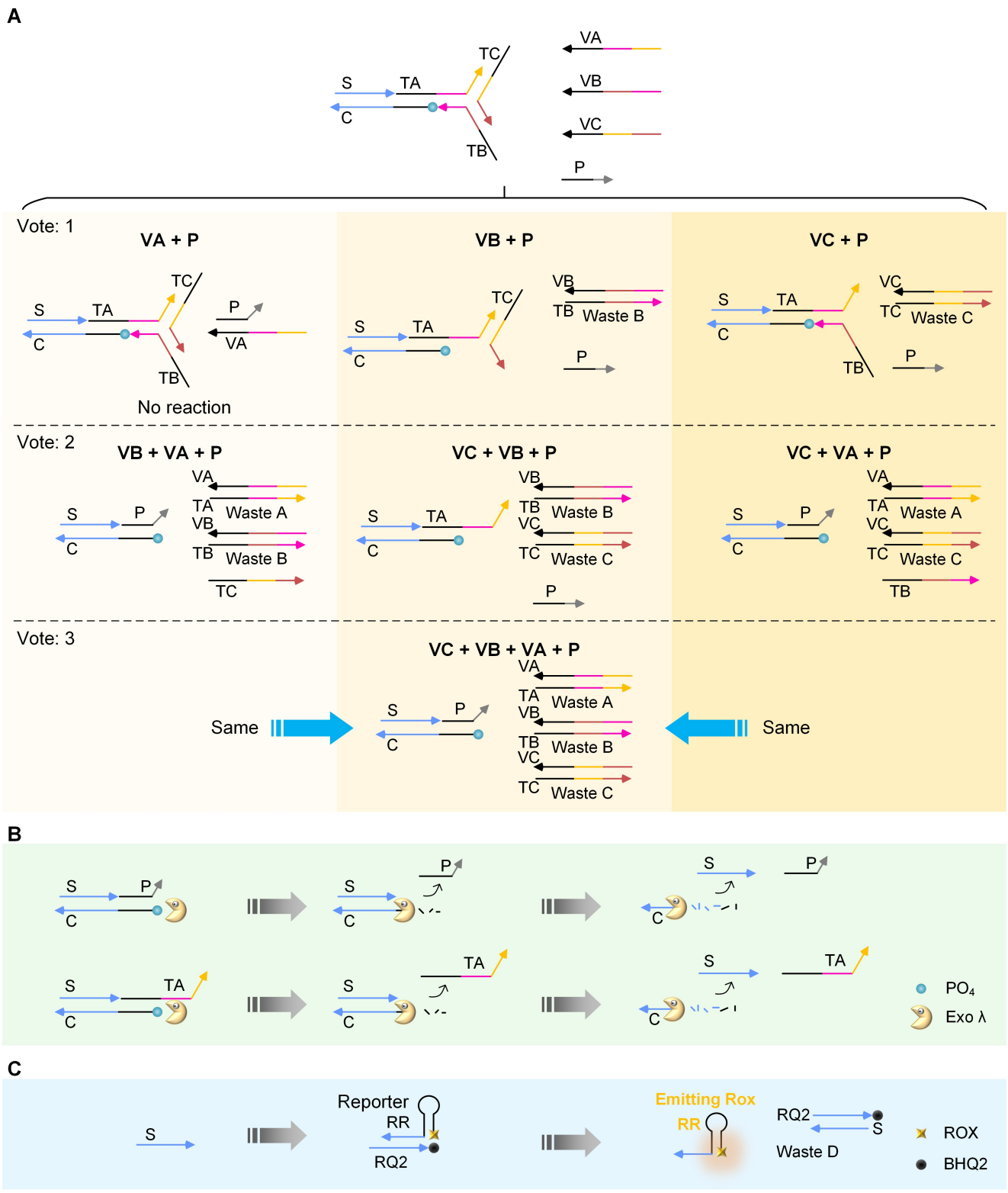

Figure S2. Schematic diagram of TDM reaction principle (related to Figure 1). (A) Strand displacement process under different voting combinations. (B) The process of Exo λ hydrolyzing two intermediate products and releasing S. (C) S triggers fluorescence excitation of the Reporter.

Strands [T~, V~] become waste products (use square brackets to represent complexes composed of 2 or more DNA strands), and P serves an auxiliary role. Upon introduction of two or more input strands, the intermediate structures [C, S, TA] or [C, S, P] form, which are then hydrolyzed by Exo λ. Subsequently, S undergoes a strand displacement reaction with the Reporter, releasing ROX-labelled RR and triggering fluorescence emission.

**Note that, due to the numerous input combinations, there are many reaction pathways that are difficult to fully display within the limited space of the main text. Therefore, detailed supplementary explanations have been provided in the SI. For the same reason, Figures S18, S20, S21, and S24 are also supplements to the principle of reaction in the main text.*

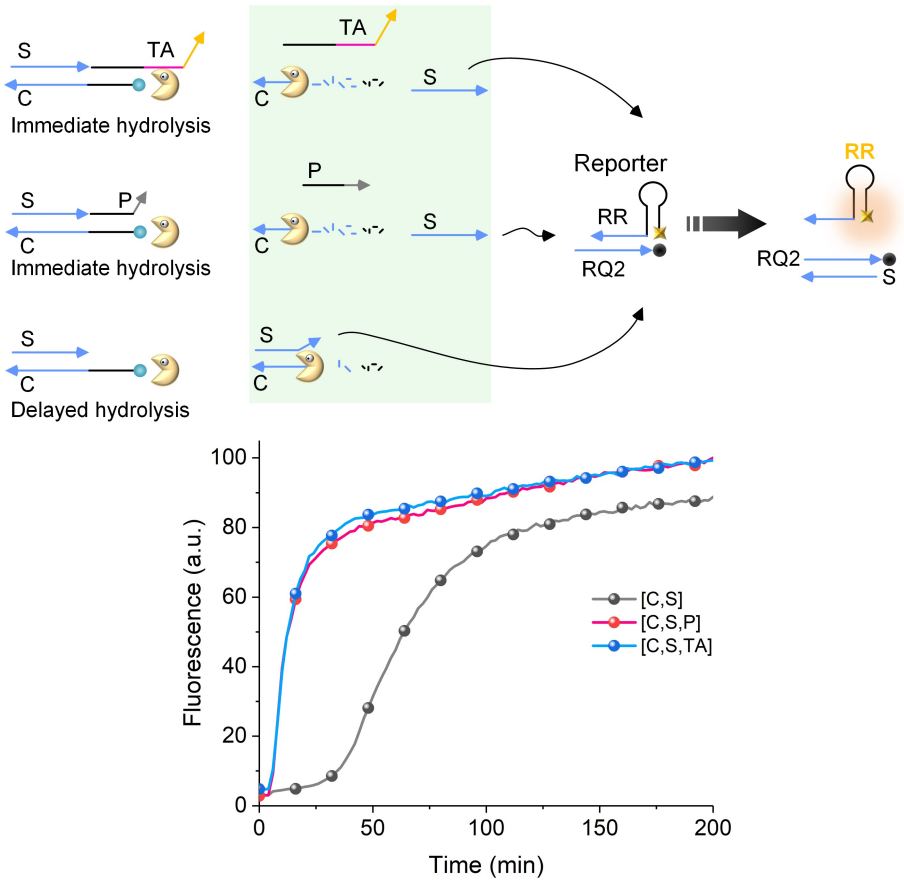

Figure S3. Comparison of hydrolysis in three intermediate structures (related to Figure 1).

Due to the characteristics of Exo λ, its hydrolysis efficiency of double stranded DNA is higher, so the fluorescence performance of [C, S, TA] and [C, S, P] is basically the same. Notably, even without the assistance of P, the intermediate products [C, S] can still undergo hydrolysis, albeit with reduced efficiency.

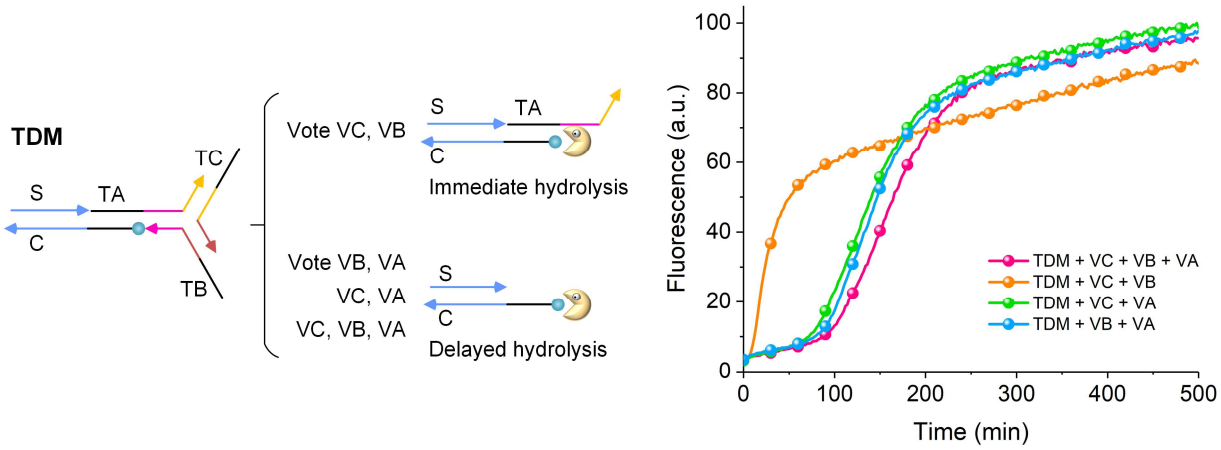

Figure S4. Voting results without P assistance (related to Figure 1).

In the absence of P assistance, only the combination of VC and VB can form intermediate structures [C, S, TA], and the hydrolysis rate is fast. The other combinations need to wait for a period of time before starting hydrolysis. Combined the research in Figure S3, we usually input P to increase the reaction rate in general experiments.

Exo λ is suitable for hydrolyzing blunt or concave ends modified with 5’ phosphate, and can also hydrolyze convex ends, but with low efficiency.

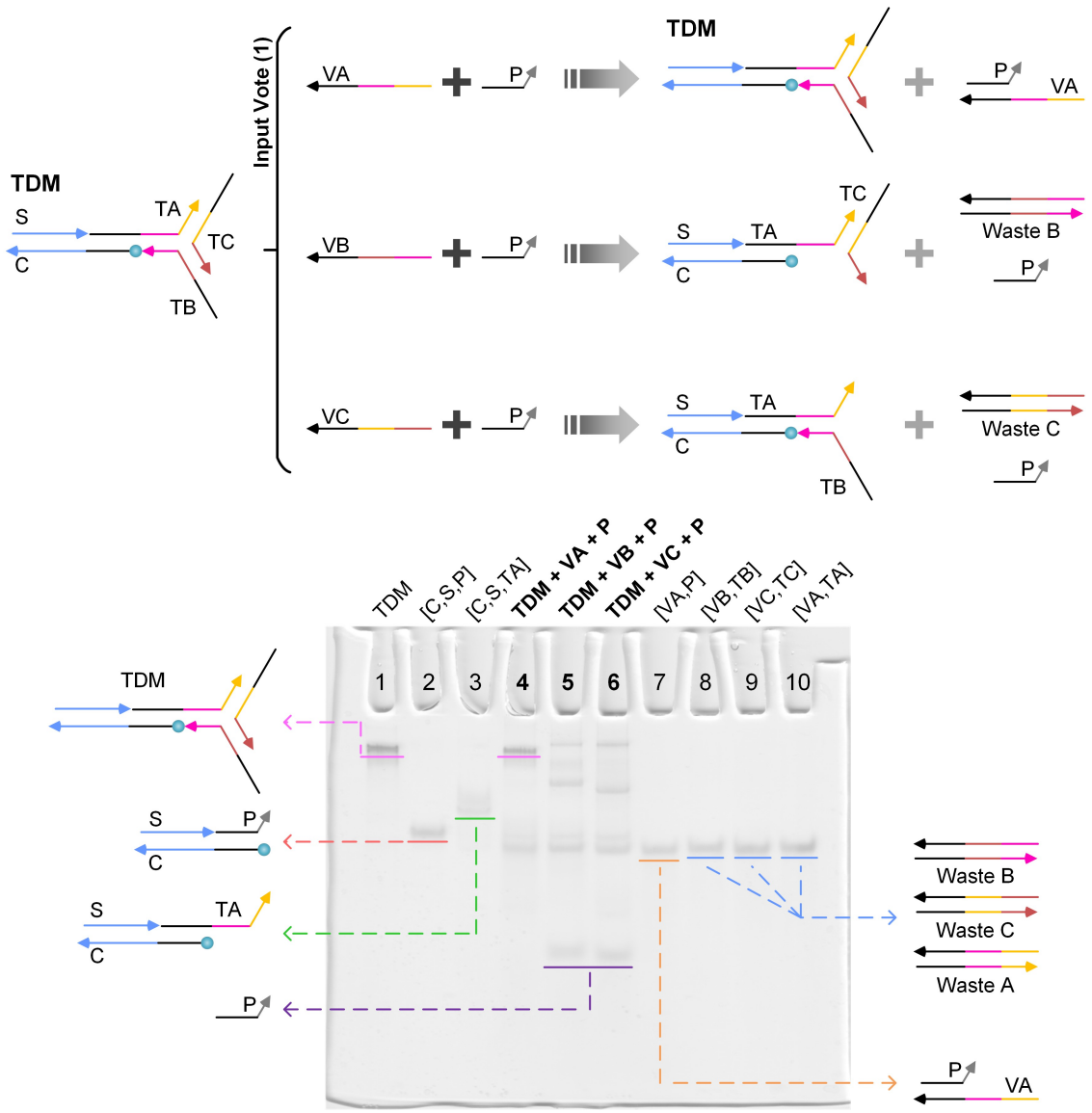

Figure S5. DNA strand displacement electrophoresis result, one vote (related to Figure 1).

Lanes 4–6 demonstrate the strand displacement reaction outcomes, while the remaining lanes serve as controls. It can be observed that no intermediate products [C, S, TA] are present, but a small amount of [C, S, P] is detected. This phenomenon may arise from the instability of the trident structure when one arm is lost, leading to partial reaction leakage. This observation also explains why in Figure 2B (main text), fluorescence shows a slight increase even when the number of votes is 1.

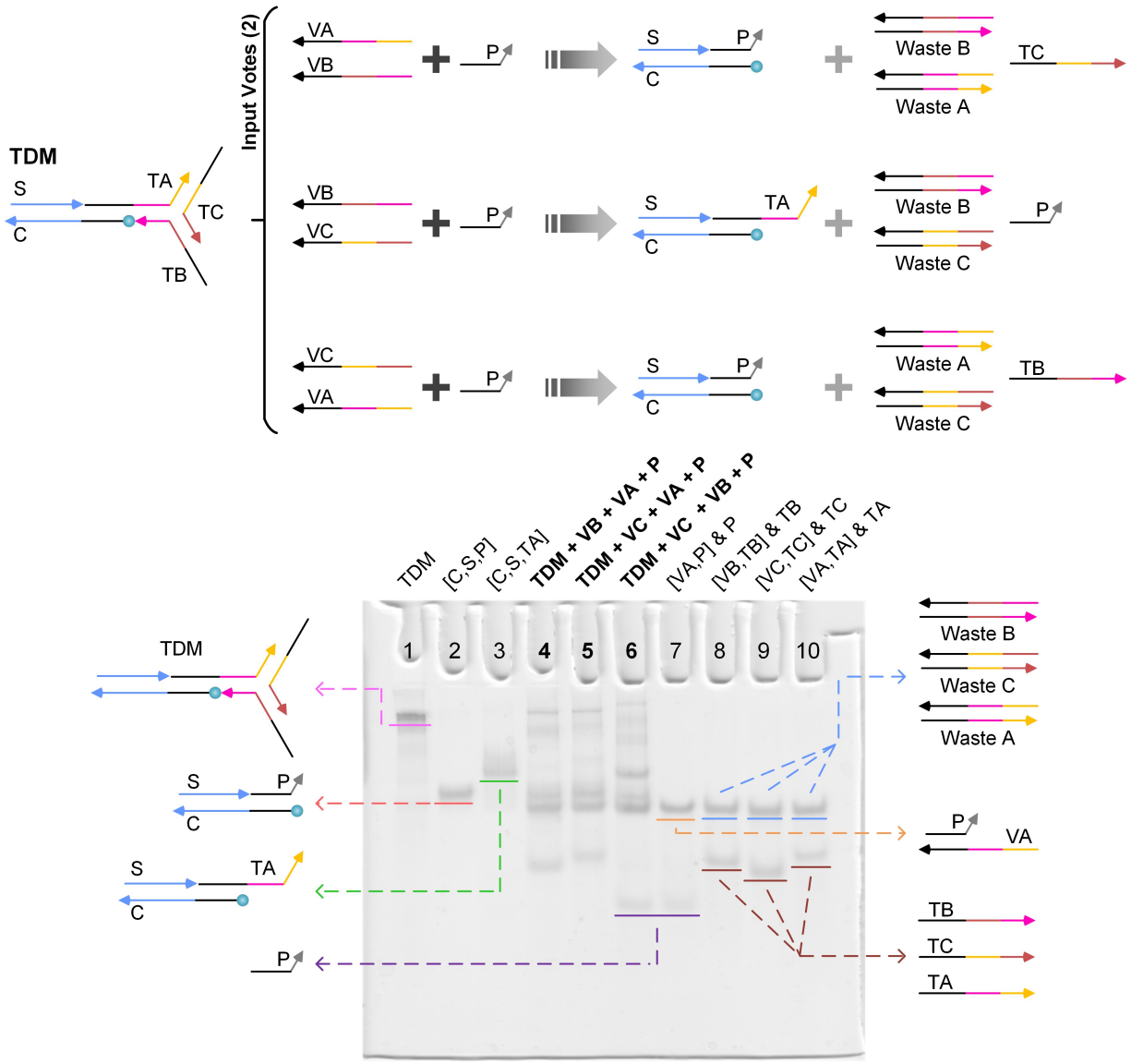

Figure S6. DNA strand displacement electrophoresis result, two votes (related to Figure 1).

Lanes 4–6 represent the results of the strand displacement reaction, while the remaining lanes are controls. It can be clearly seen that after the strand displacement reaction, two key intermediate products [C, S, TA] and [C, S, P] are produced, which will be hydrolyzed by Exo λ in the subsequent process.

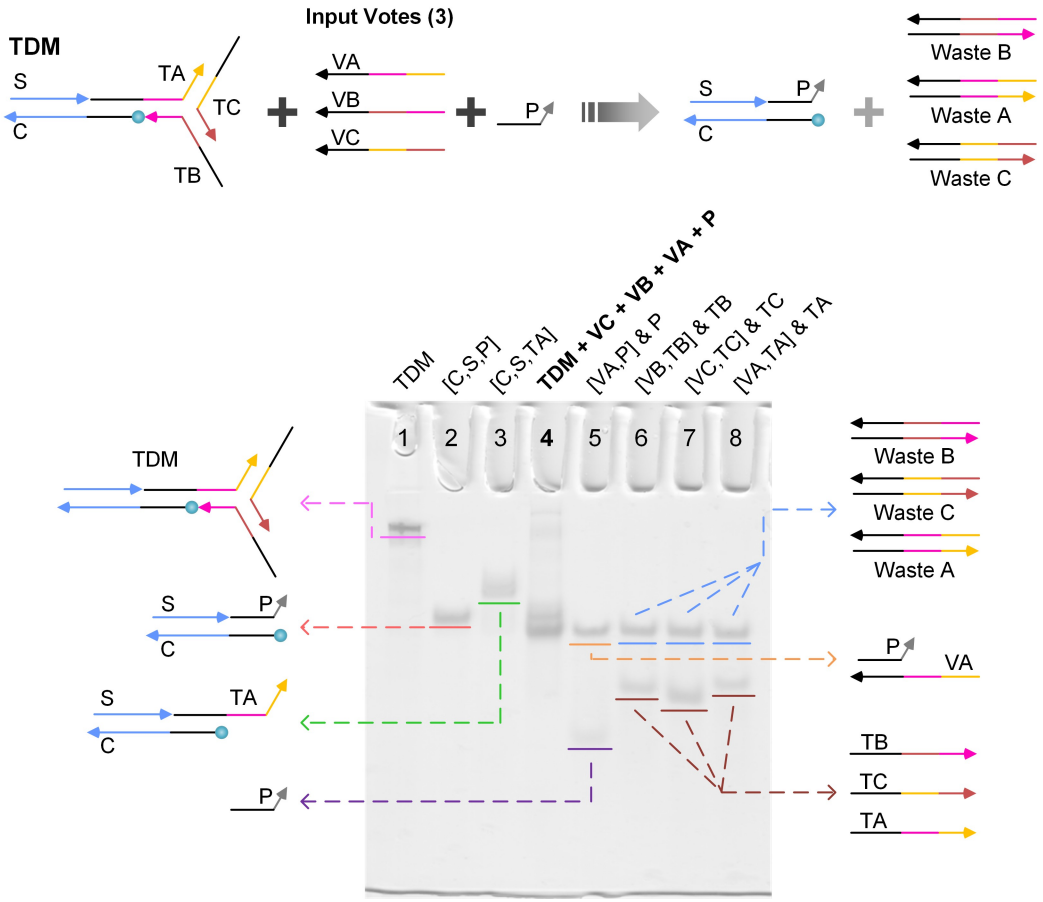

Figure S7. DNA strand displacement electrophoresis result, three votes (related to Figure 1).

Lane 4 represent the results of the strand displacement reaction, while the remaining lanes are controls. When the process involves three votes, only the intermediate products [C, S, P] are formed. The [C, S, TA] is almost non-existent. [C, S, P] will be hydrolyzed in subsequent operations.

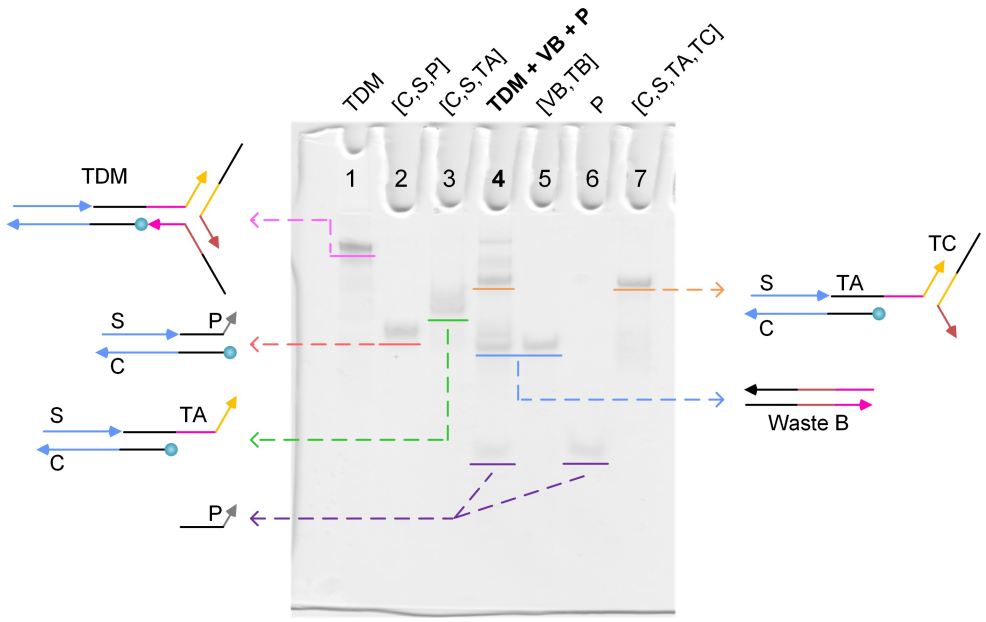

Figure S8. DNA strand displacement electrophoresis result, vote VB, with more control lanes (related to Figure 1).

Lane 4 represent the results of the strand displacement reaction, while the remaining lanes are controls. Take voting VB as an example to add the bands not described in the previous gel.

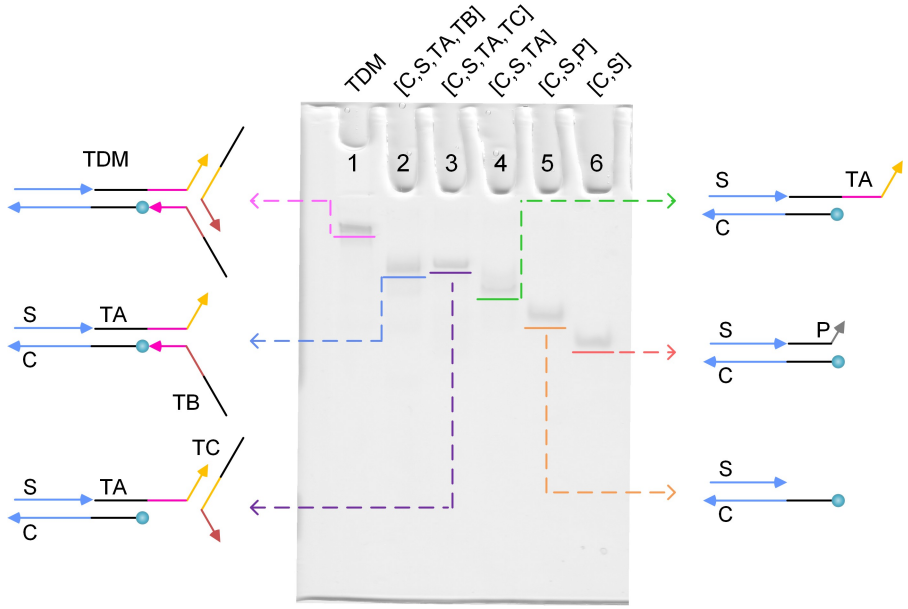

Figure S9. The distinction of six structures containing S in different lanes (related to Figure 1).

Supplement to the ingredients not described in the previous gel.

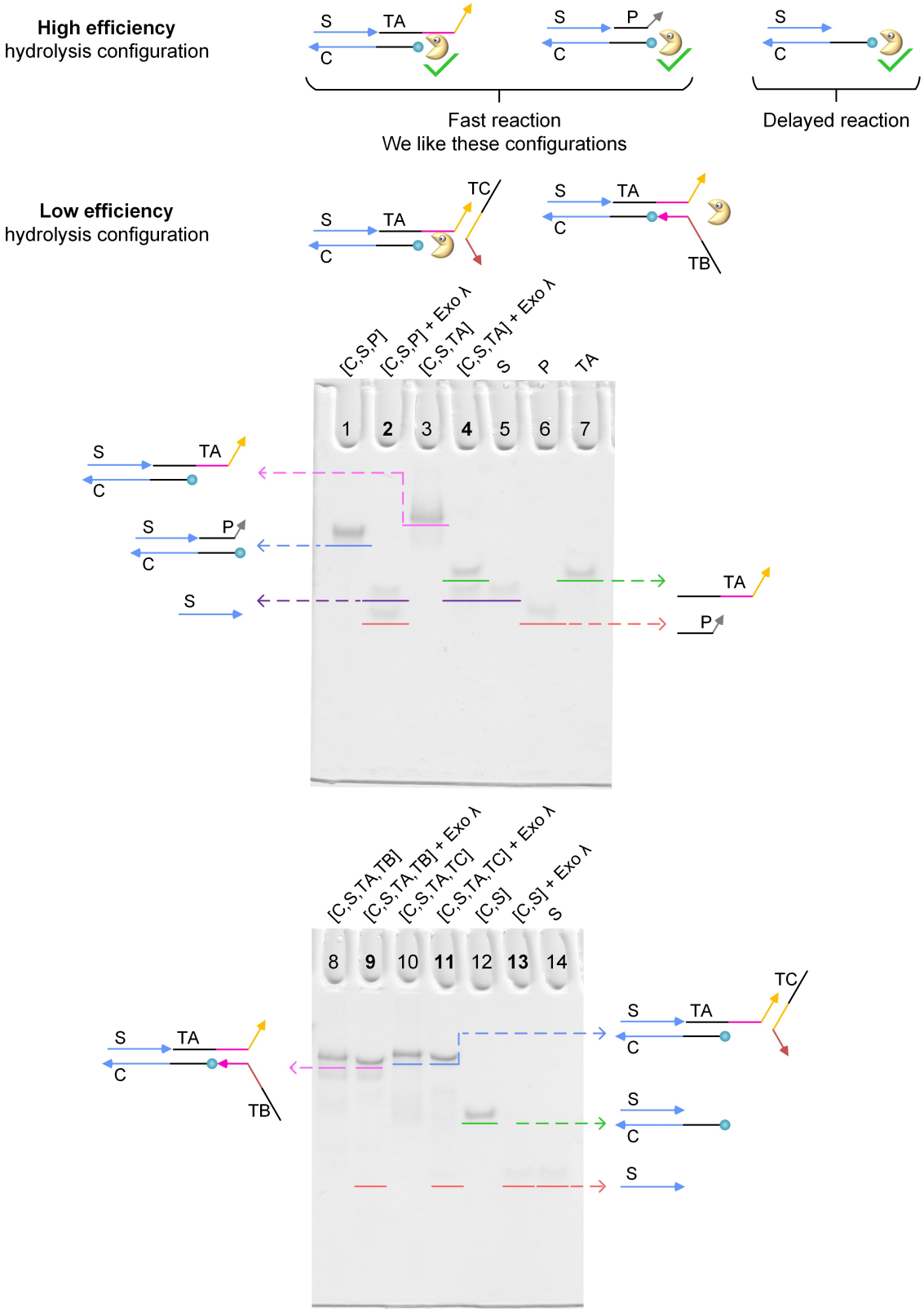

Figure S10. Electrophoresis of high/low efficiency hydrolysis configuration (related to Figure 1).

In the efficient hydrolysis configuration (Lanes 2, 4, and 13), substantial amounts of strand S were released, whereas only minimal S was produced in the inefficient configuration (Lanes 9 and 11). The complexes [C, S, TA, TB] and [C, S, TA, TC], formed with only one affirmative vote, both exhibited significant hydrolysis resistance. Notably, [C, S, TA, TC] (lane 11) maintained this resistance even while partially exposing phosphate sites, as confirmed by the gel electrophoresis results.

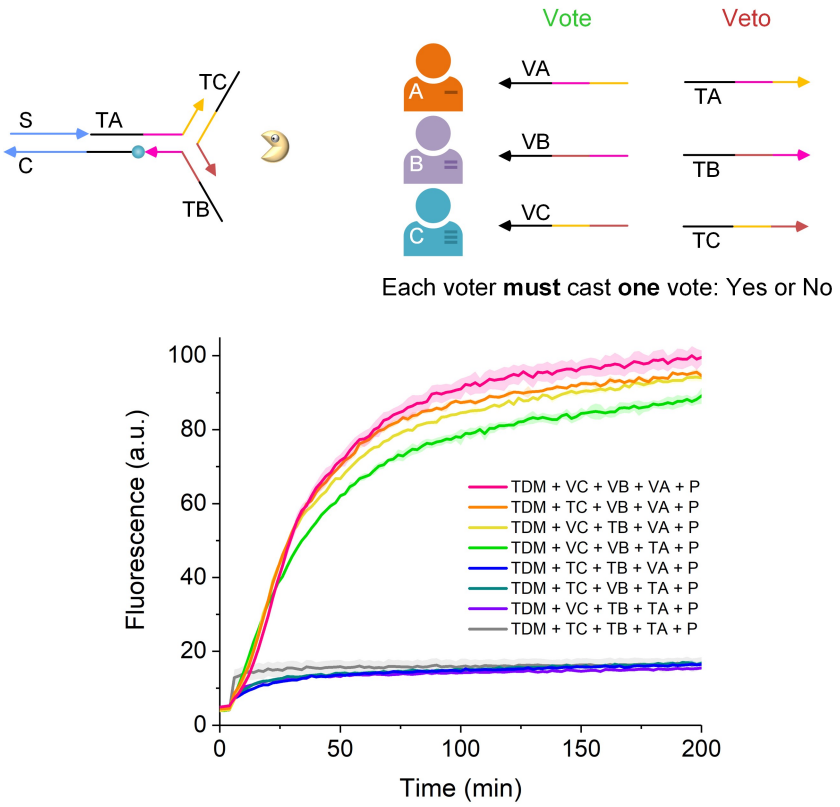

Figure S11. TDM mechanism with vetoes (related to Figure 1).

In Figure 1 of the main text, we define input V~ as voting, while no input is considered abstention. Here, we further define T~ as a veto vote. When it is the players' turn to decide, they must cast one vote and cannot abstain. Fluorescence results confirm that the majority rule principle remains unchanged. One veto vote is not enough to affect the approval vote of the two-person alliance.

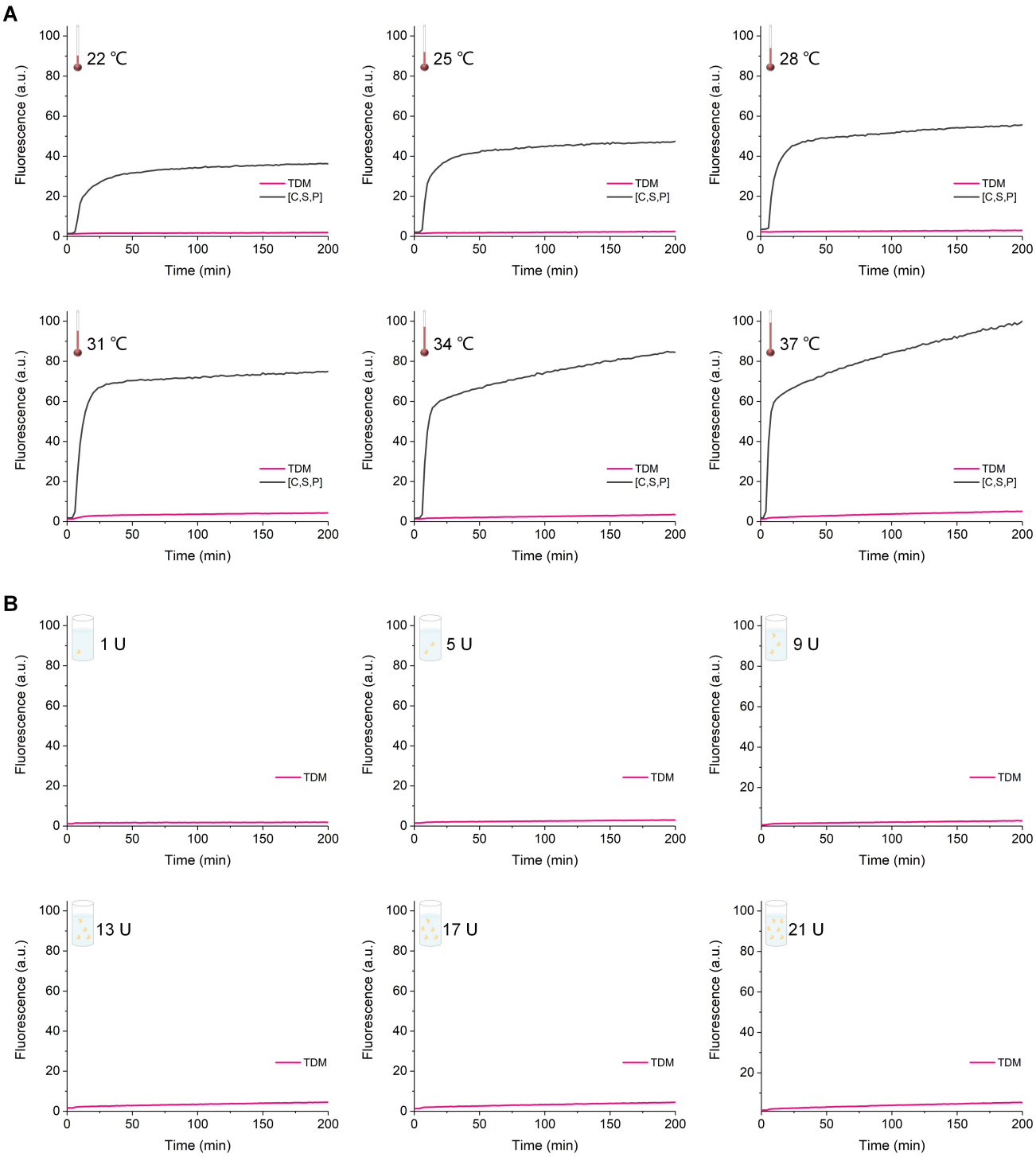

Figure S12. The influence of temperature and Exo λ concentration on TDM. (A) Temperature, 22–37 ℃. (B) concentration, 1–21 U (related to Figure 1).

Under varying temperatures and Exo λ concentrations, TDM demonstrates strong resistance to hydrolysis, attributed to the trident structure's large size (>3 nm). TDM exhibits high stability and is expected to persist in the environment for extended periods.

In addition, we observed that when the temperature exceeded 34°C, the hydrolysis fluorescence curves of [C, S, P] differed somewhat from those at lower temperatures. Not only was the fluorescence growth rate exceptionally fast in the initial stage, but it also continued to show an increasing trend in the later phase. Here we propose two hypotheses to explain this phenomenon.

Hypothesis 1 (enzyme kinetics & substrate depletion): At higher temperatures, Exo λ exhibits significantly enhanced activity, leading to the rapid hydrolysis of the abundant [C, S, P] substrates at the initial reaction stage (evidenced by the steep initial slope). This depletes the majority of the substrate pool. Subsequently, the remaining low concentration of [C, S, P] structures has a reduced probability of enzyme encounter, resulting in the slower observed rate in the later phase.

Hypothesis 2 (substrate stability & altered specificity): Elevated temperature may induce partial thermal destabilization of the [C, S, P] structure, causing the P to dissociate prematurely and generate [C, S] complexes with a 5'-convex end. While Exo λ hydrolyzes such convex ends with lower efficiency compared to blunt or recessed ends, it retains some activity. Therefore, the later phase likely reflects this slower efficient hydrolysis of the altered substrate population.

These mechanistic interpretations are consistent with the known biochemical properties of Exo λ, and are presented as our current understanding of the temperature-dependent kinetics.

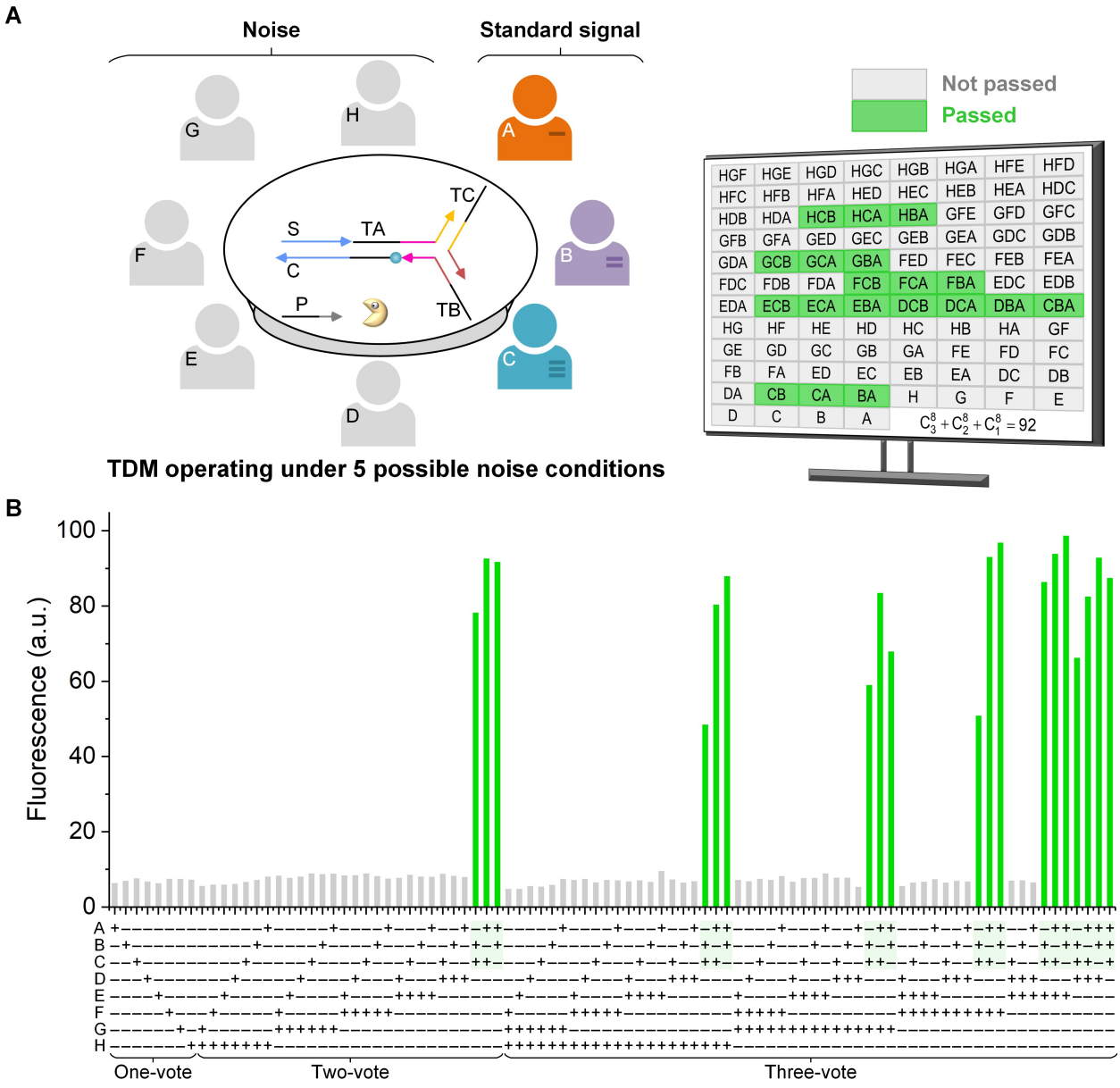

Figure S13. The impact of interference signals on TDM decision results. (A) A to C are standard input signals, and D to H are noise signals. (B) Fluorescence results with voting numbers ranging from 1 to 3 (related to Figure 1).

We introduced 5 non-standard input signals as noise, and TDM allows a maximum of 3 signals to be input at a time, resulting in a total of 92 combinations ($C_3^8 + C_2^8 + C_1^8 = 92$). The system generated fluorescence only when any of the following: {A, B}, {B, C}, {A, C}, {A, B, C}, {A, B, X}, {B, C, X}, and {A, C, X} (where X represents any player from D to H). All other combinations failed to trigger fluorescence, meaning that the decision was not passed. The experimental results indicate that in the presence of noise, there may not be significant interference with the operation of TDM. The noise DNA sequences used are shown in the Table S3.

The real-time fluorescence curves of 92 independent experiments are shown in Figures S14–S17.

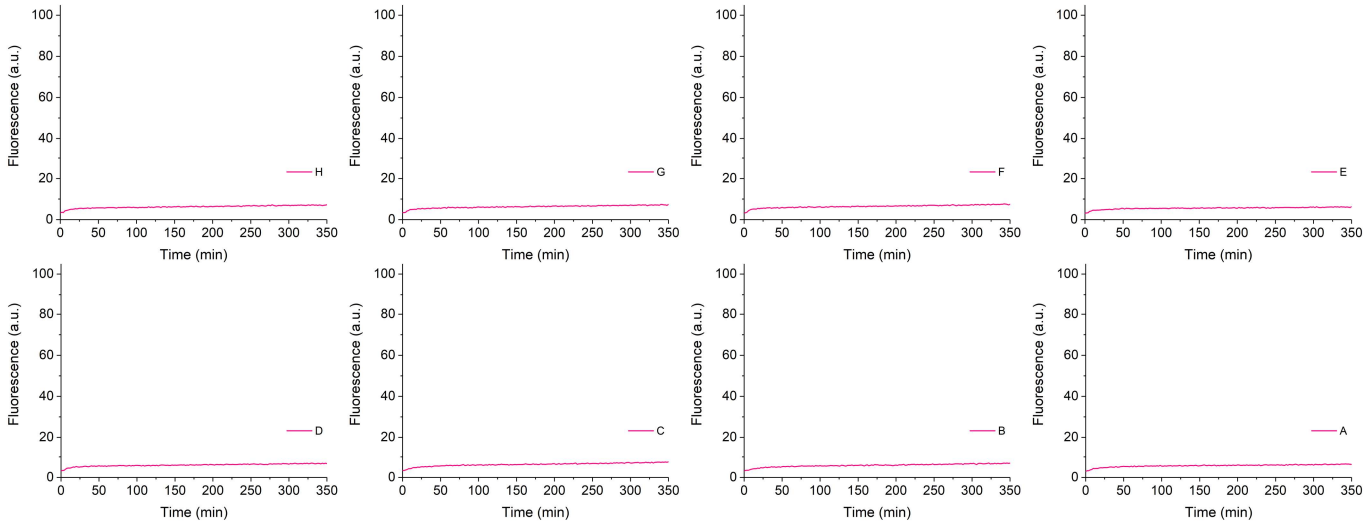

Figure S14. Real-time fluorescence of one vote for Figure S13 (related to Figures 1 and S13).

Results VA–VH are abbreviated A–H. The decision failed with only one vote (fluorescence not excited).

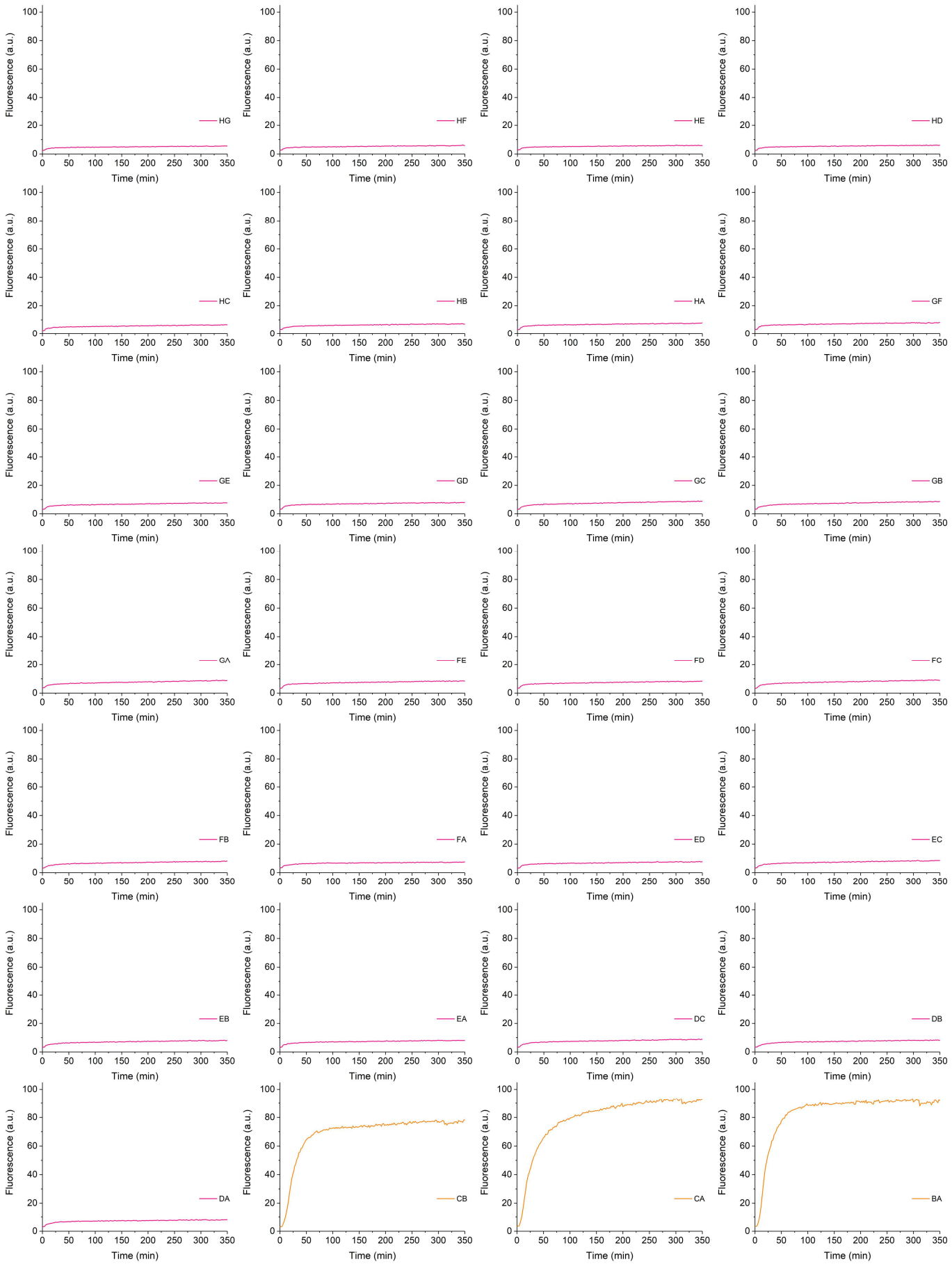

Figure S15. Real-time fluorescence of two votes for Figure S13 (related to Figures 1 and S13).

Only three standard signal combinations ({C, B}, {C, A}, and {B, A}) led to the decision being passed.

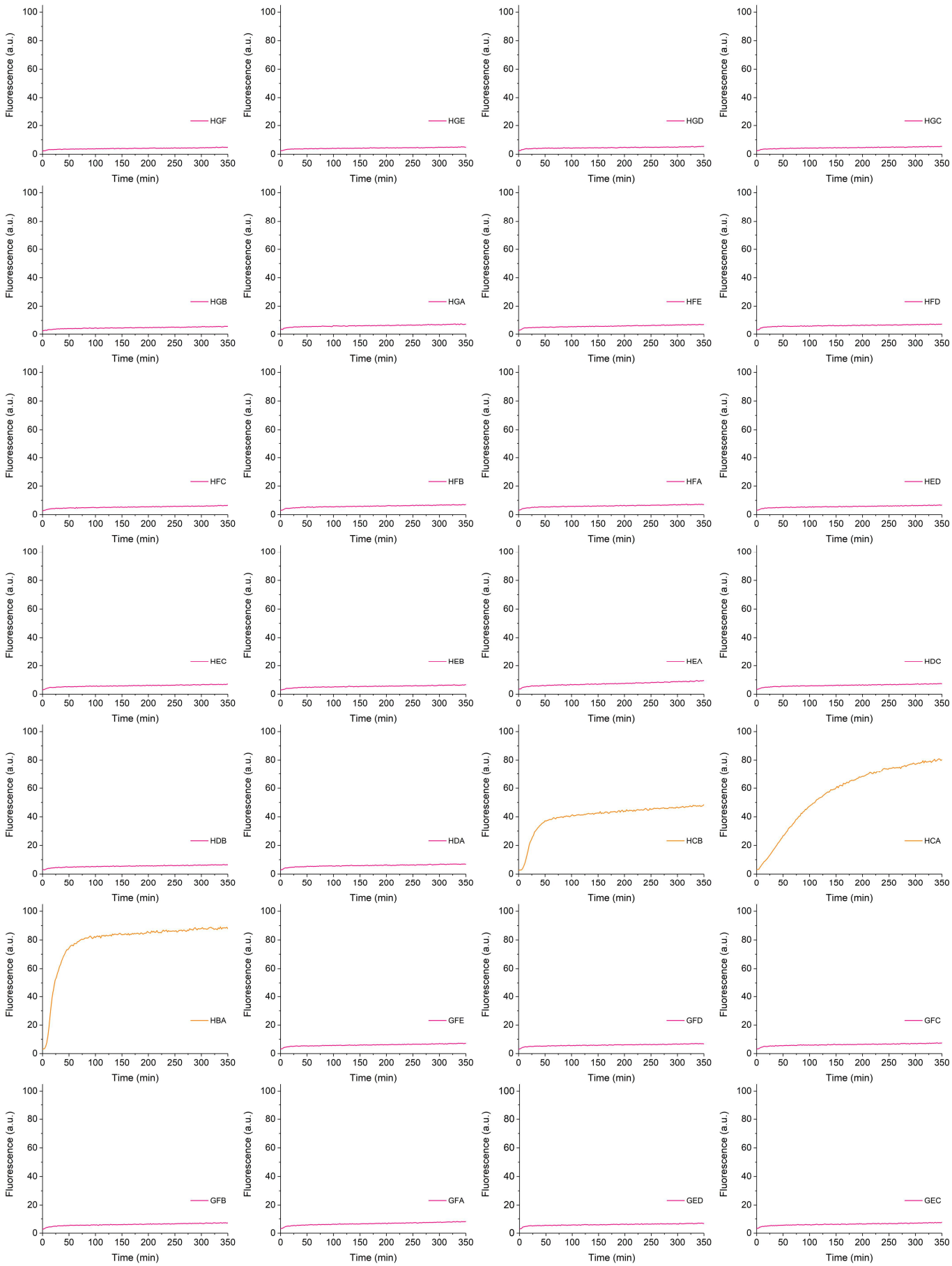

Figure S16. Real-time fluorescence of three votes for Figure S13, part 1 (related to Figures 1 and S13).

A decision can be passed only if the voting combination includes {C, B, X}, {C, A, X}, or {B, A, X} (X represents any D–H). There are at least two standard signals.

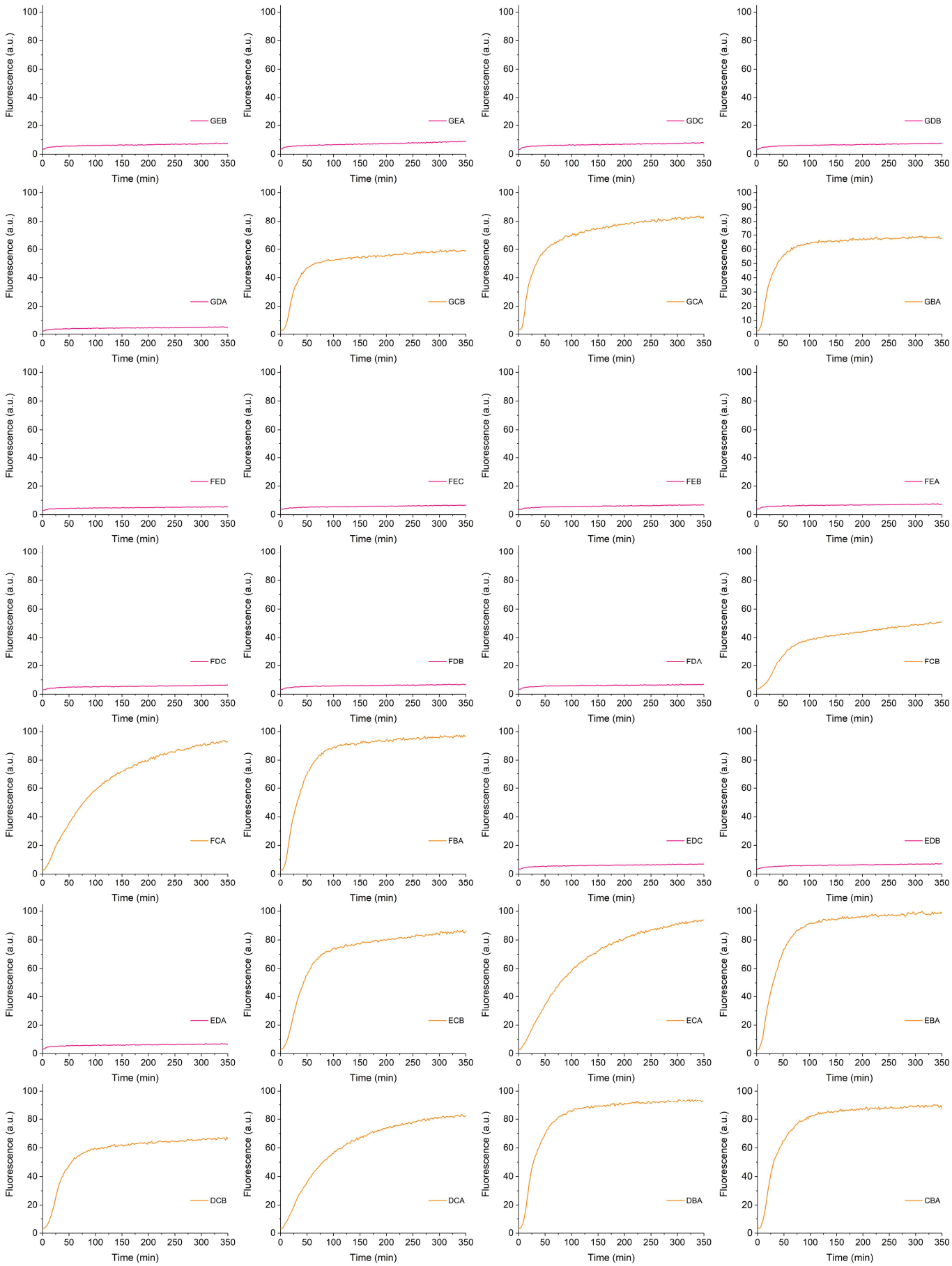

Figure S17. Real-time fluorescence of three votes for Figure S13, part 2 (related to Figures 1 and S13).

Same as Figure S16, to pass the decision, the combination must include any two standard signals of C, B, or A.

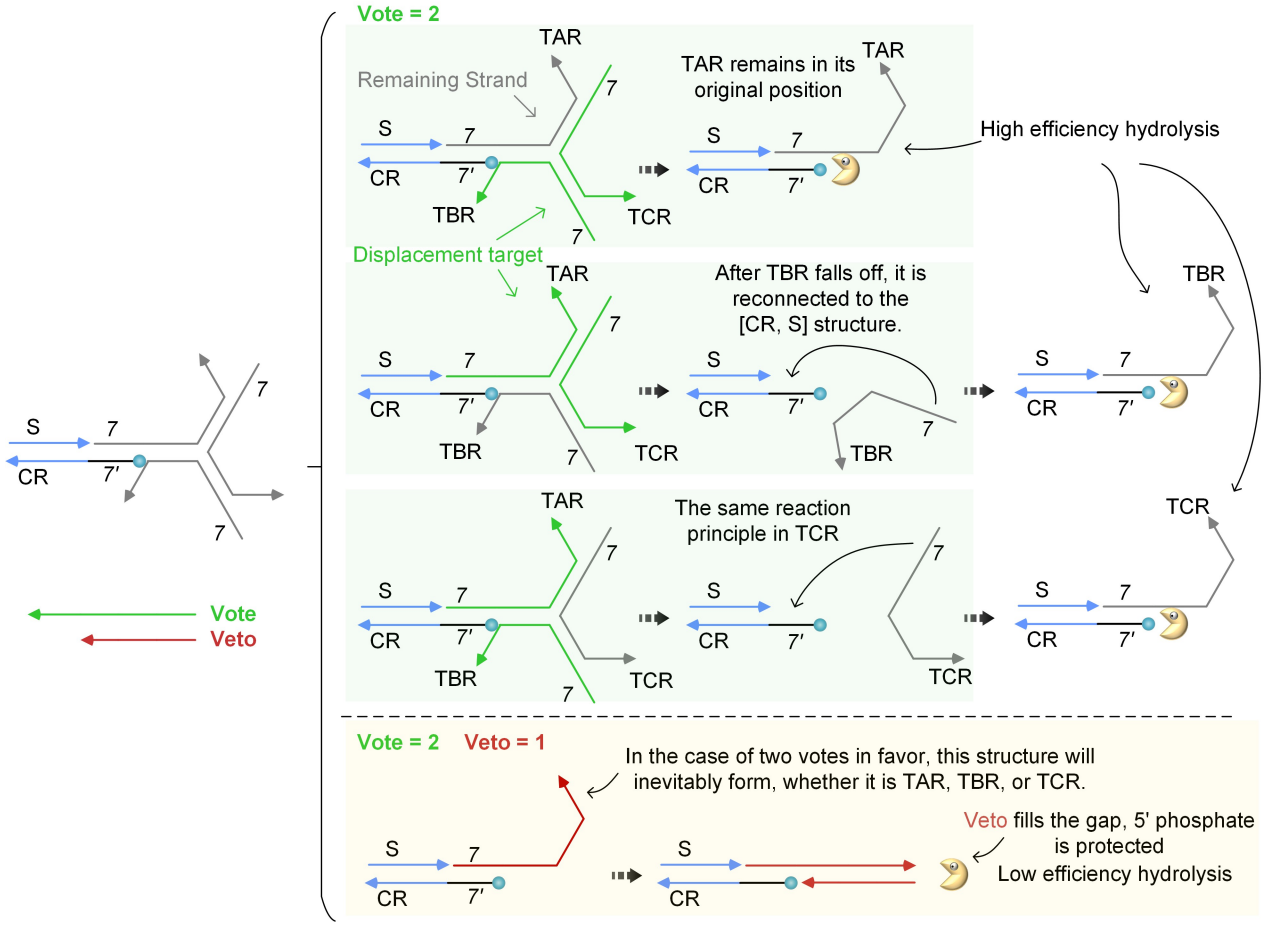

Figure S18. Principle of one-vote veto system (related to Figure 3).

With two votes in favor and due to the shared common domain 7, regardless of which two arms of the trident structure are displaced, the system tends to revert to the [CR, S, TXR] configuration (X ∈ {A, B, C}). Forming an efficient hydrolysis configuration. Subsequently, the veto sealed the concave 5' end, forming an inefficient hydrolysis structure.

When the number of affirmative votes is 2, if DNA strand displacement reaction is performed on TBR and TCR, TAR will not be affected and will remain in its original position.

If DNA strand displacement reaction is performed on TAR and TCR, TBR loses its connection with CR and will first detach from the structure. Subsequently, due to the existence of domain 7 in TBR, it will reconnect with CR through domain 7.

If DNA strand displacement reaction is performed on TAR and TBR, TCR will lose its connection with CR and also detach from the structure first. Subsequently, based on the same principle as TBR, it will reconnect with CR through domain 7.

Therefore, in the case of two votes in favor, there will ultimately be a tendency to form a structure with a 5' concave end with CR. And the veto can just fill this concave end, preventing the 5' phosphate site from being exposed and losing its ability to be hydrolyzed by Exo λ. So, S will not be released.

TAR, TBR, and TCR all have 7 domains, so as shown in the main text, there are three possible ways to connect with [CR, S]. This Figure illustrates the case where TAR is directly connected to [CR, S]. The other two connection methods also have similar reaction processes.

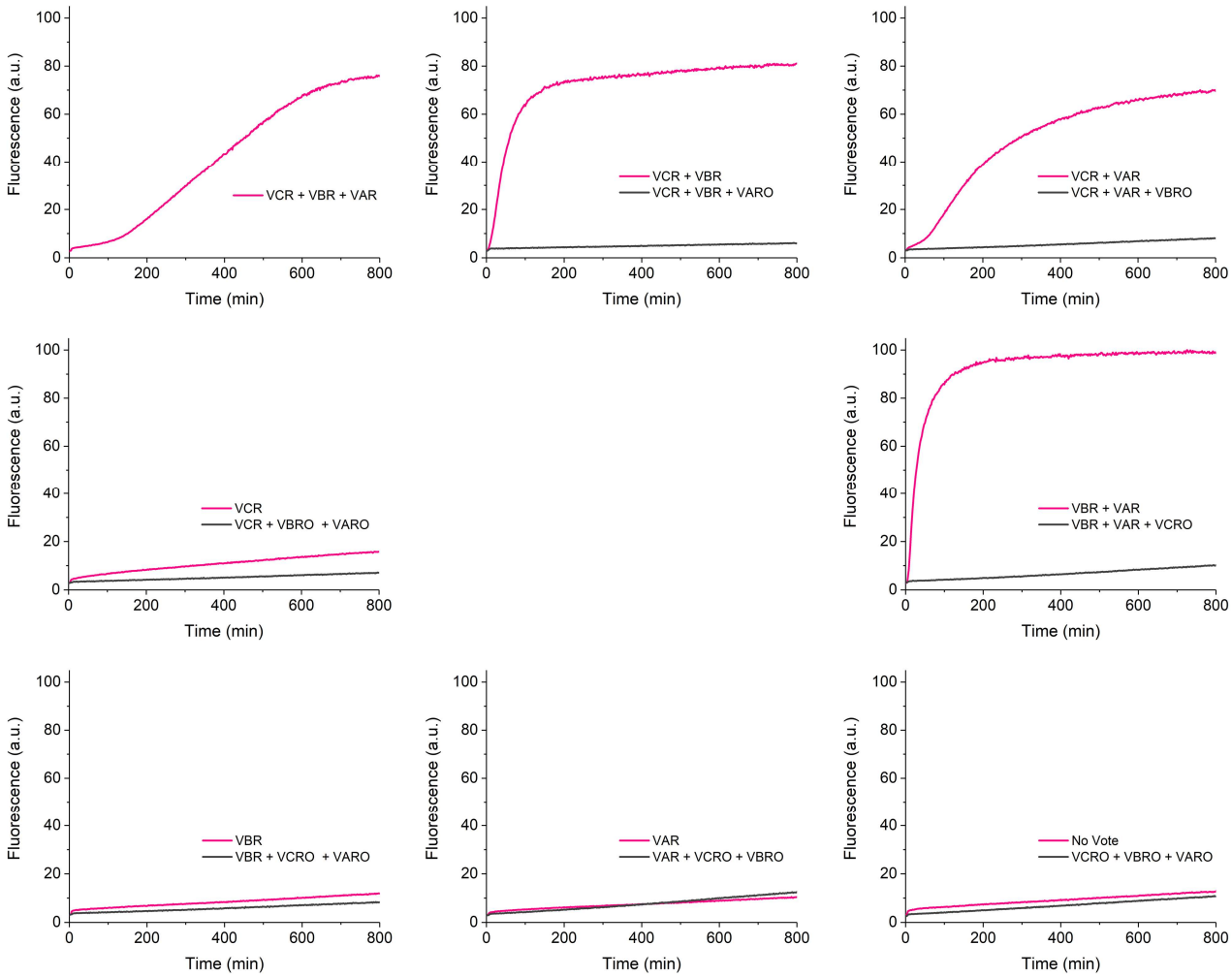

Figure S19. Real-time fluorescence of one-vote veto system (related to Figure 3).

These plots show the real-time fluorescence data corresponding to the bar chart in Figure 3 of the main text. After using a veto, fluorescence showed significant inhibition. Fluorescence excitation can only occur without a veto vote.

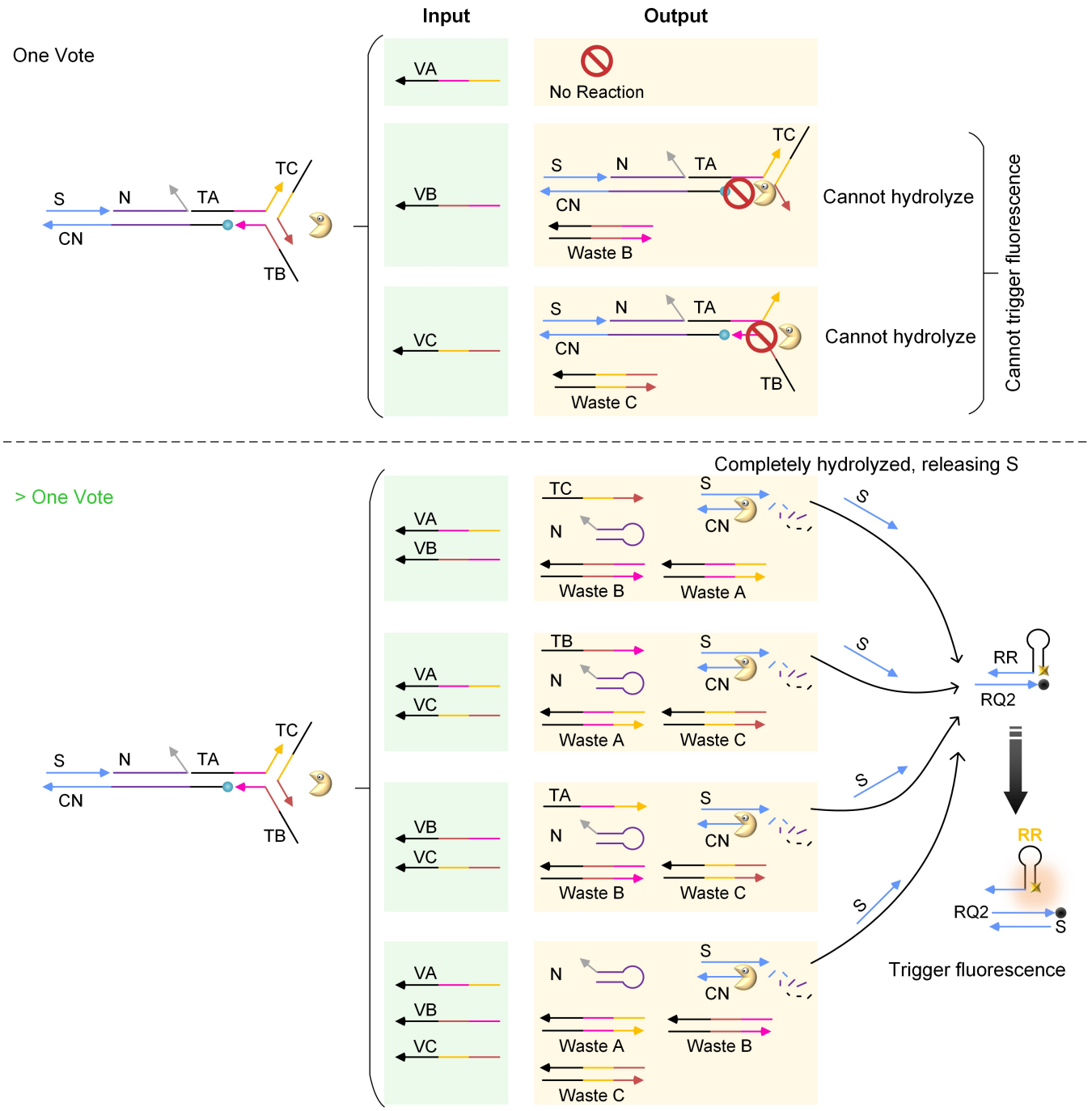

Figure S20. Schematic diagram of TDM-A1 reaction principle (related to Figure 4).

In the TDM-A1 configuration, the DNA strand displacement and hydrolysis processes are essentially identical to those in the original TDM system. The only difference is that an additional N is released.

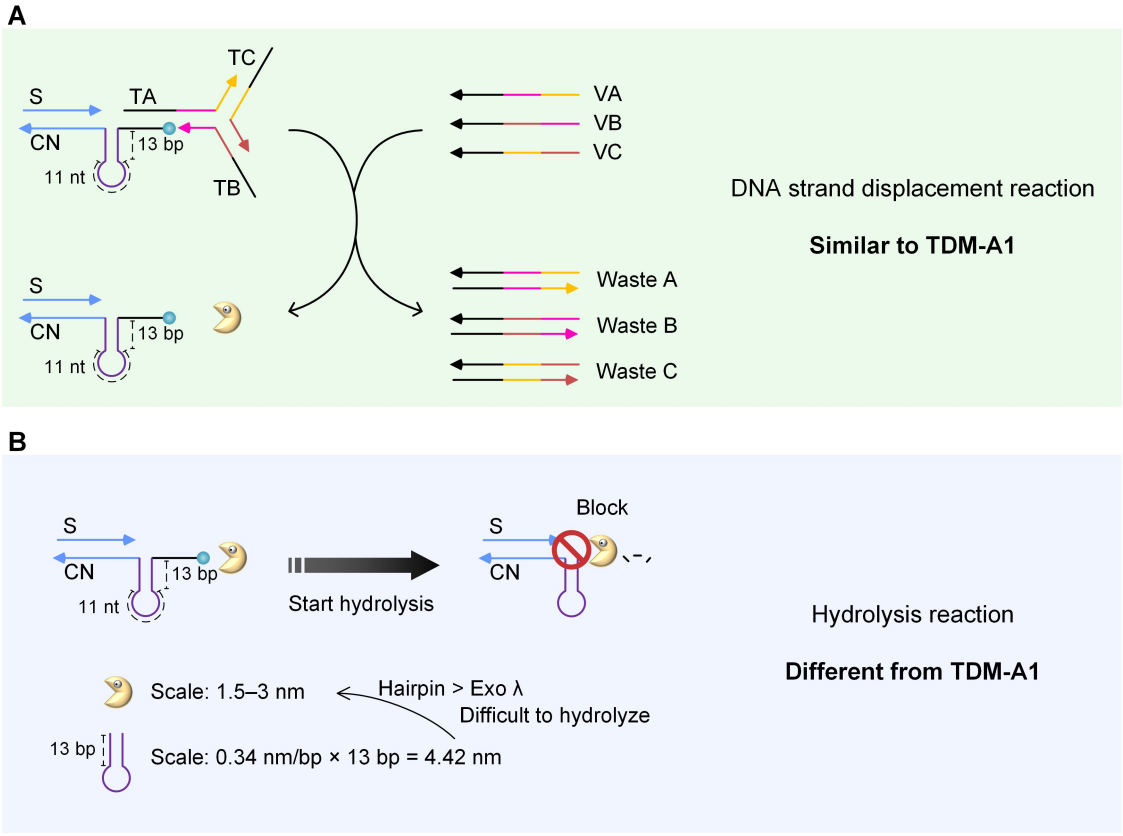

Figure S21. Schematic diagram of TDM-A2 reaction principle (related to Figure 4). (A) Strand displacement reaction. (B) Hydrolysis reaction.

Using the same DNA strand displacement reaction, we observed that during hydrolysis, the size of Exo λ is smaller than that of the hairpin in TDM-A2. This large scale of hairpin causes Exo λ to get stuck and unable to proceed, thereby preventing further hydrolysis.[1, 2] This mechanism explains why fluorescence growth ceases immediately upon administrator intervention.

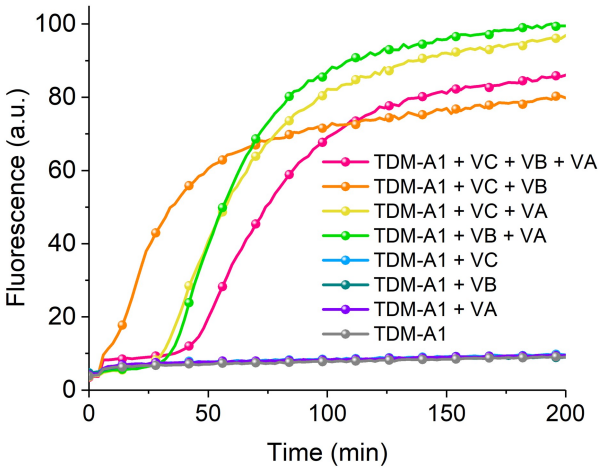

Figure S22. The complete voting result when the administrator does not veto (related to Figure 4).

The strategy maintained fluorescence characteristics similar to those of the original TDM scheme, with significant positive and negative controls. Fluorescence emission occurs only when two or more votes are present.

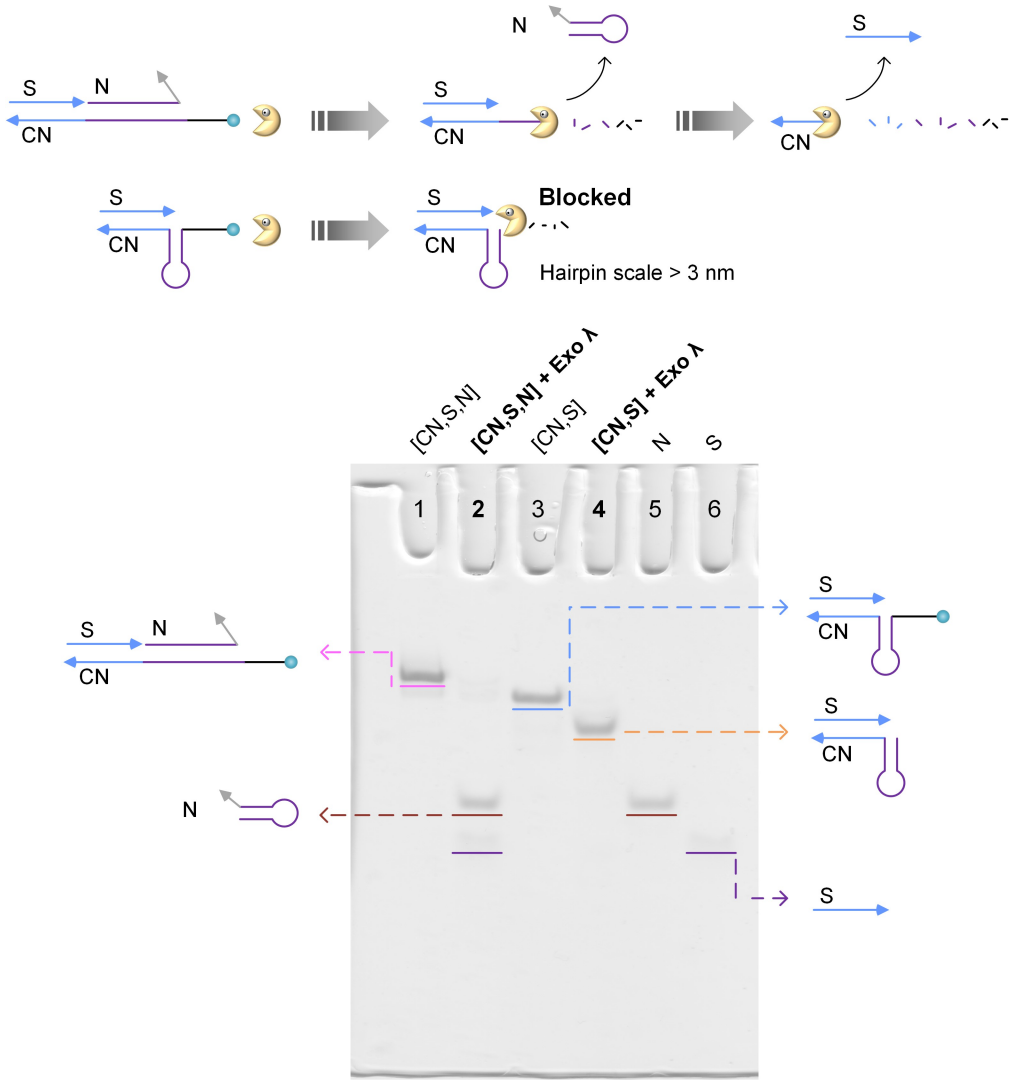

Figure S23. Electrophoretic results of TDM-A2 (without trident) hydrolysis (related to Figure 4).

In Lane 2, it can be clearly seen that the [CN, S, N] structure is hydrolyzed, producing two fragments: S and N. In Lane 4, Exo λ can only partially invade the [CN, S] region, while the remaining part is protected by Hairpin,[2] making further hydrolysis difficult and thus preventing the production of S.

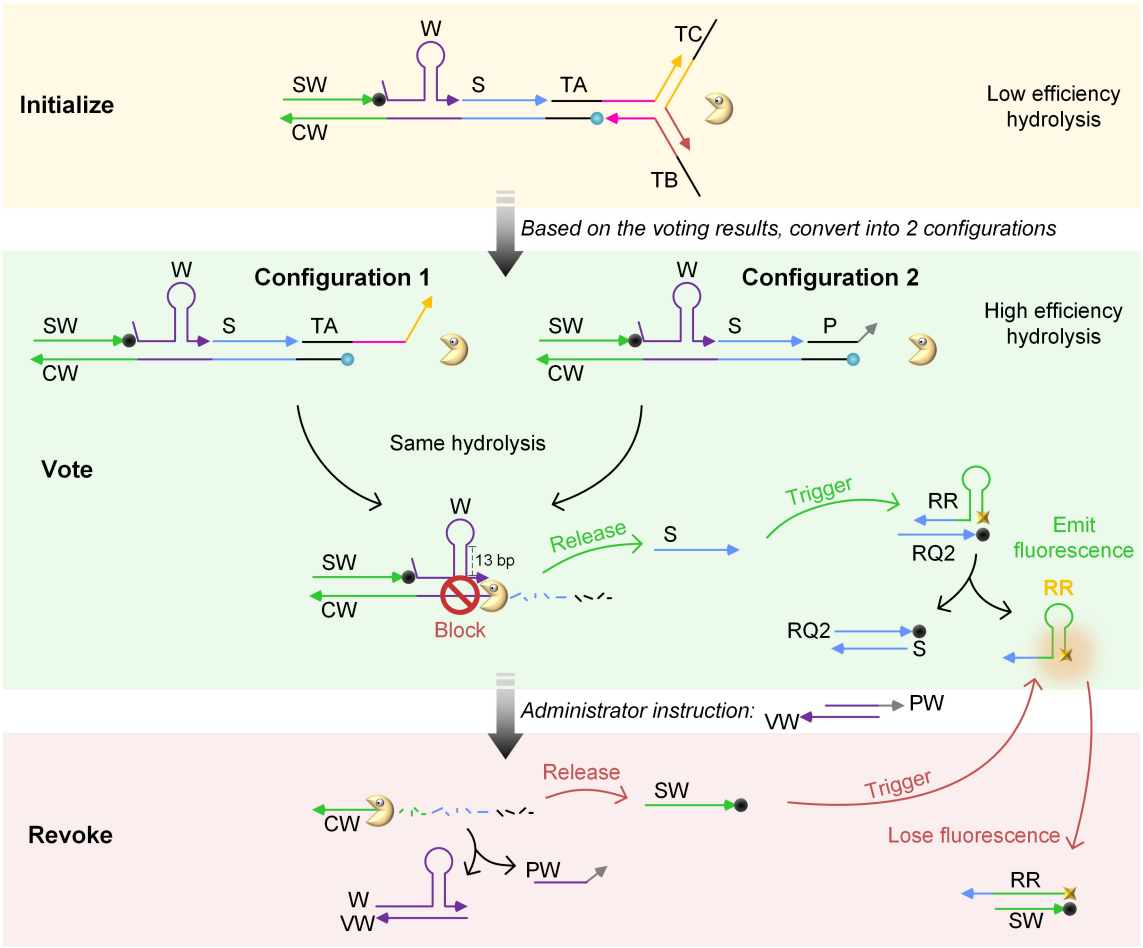

Figure S24. Revocation principle (related to Figure 5).

The previous process remains consistent with the original principle, and S is effectively released, while the remaining portion was blocked by the W hairpin (stem length: 13 bp, >3 nm) and could not proceed with hydrolysis. Signal S then activates the Reporter unit, producing fluorescence. Upon issuing the revocation command, W is removed *via* a DNA strand displacement reaction. The remaining structure resumes hydrolysis and releases signal SW, which carries a BHQ2 quencher and is complementary to the fluorescence-emitting reporter (RR). Through resonance energy transfer, SW absorbs the ROX fluorescence, leading to macroscopic fluorescence quenching and thus the revocation of the decision.

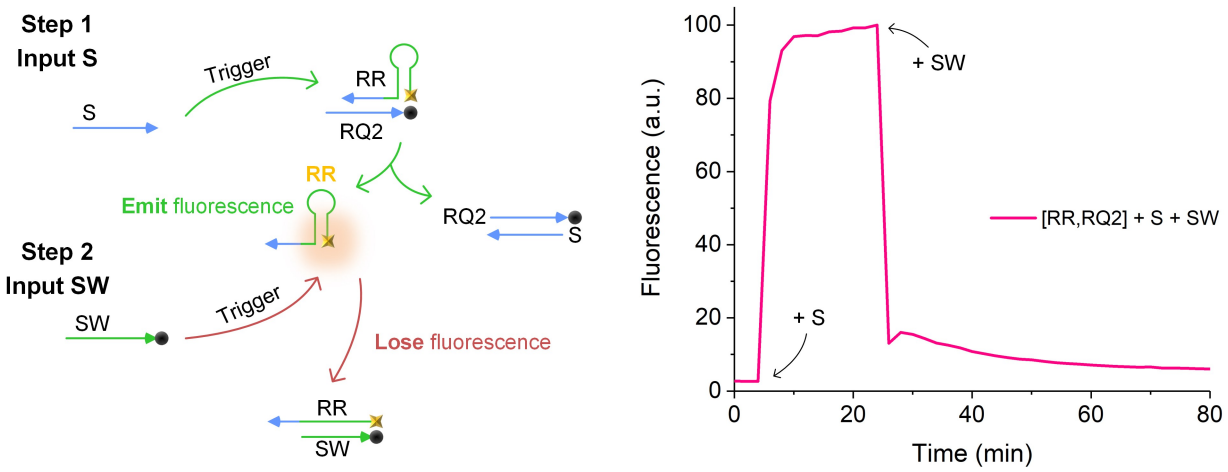

Figure S25. Fluorescence reaction in revocation principle (related to Figure 5).

This is the fluorescence result from separately testing the Reporter unit and the two input signals (S and SW). Upon the input of S, the fluorescence increased rapidly and reached a steady state, indicating sufficient separation between RR and RQ2. Subsequently, when SW was inputted, the fluorescence decreased immediately and stabilized, suggesting stable binding between RR and SW and resulting in fluorescence quenching.

Reference

1. X. Zhang, X. Liu, X. K. Zhang, S. Cui, Y. Yao, B. Wang and Q. Zhang, *ACS Appl. Mater. Interfaces*, 2024, **16**, 24372–24383.
2. Y. Yao, X. Zhang, X. Liu, X. K. Zhang, B. Wang and Q. Zhang, *ACS Nano*, 2025, **19**, 24763–24772.